Eur. Phys. J. Appl. Phys. (2015) 69: 11001
DOI: 10.1051/epjap/2014140254

THE EUROPEAN PHYSICAL JOURNAL
APPLIED PHYSICS

Regular Article

An "intelligent" approach based on side-by-side cascade-correlation neural networks for estimating thermophysical properties from photothermal responses

Stéphane Grieu[1], Olivier Faugeroux[1], Adama Traoré[1], Bernard Claudet[1], and Jean-Luc Bodnar[2,a]

[1] PROMES, Université de Perpignan Via Domitia, 52 avenue Paul Alduy, 66860 Perpignan, France
[2] GRESPI/ECATHERM, Université de Reims Champagne-Ardenne, BP 1039, 51687 Reims, France

Received: 20 June 2014 / Received in final form: 9 October 2014 / Accepted: 2 December 2014
Published online: 7 January 2015 –

Abstract. In the present paper, an artificial-intelligence-based approach dealing with the estimation of thermophysical properties is designed and evaluated. This new and "intelligent" approach makes use of photothermal responses obtained when subjecting materials to a light flux. So, the main objective of the present work was to estimate simultaneously both the thermal diffusivity and conductivity of materials, from front-face or rear-face photothermal responses to pseudo random binary signals. To this end, we used side-by-side feedforward neural networks trained with the cascade-correlation algorithm. In addition, computation time was a key point to consider. That is why the developed algorithms are computationally tractable.

1 Introduction

The photothermal experiment consists in subjecting material samples to a light flux. As a result, light absorption causes a local elevation of temperature. So, the front-face or rear-face photothermal response is proportional to the surface temperature of the considered sample and dependent on its thermophysical properties, its structure and the presence of defects or delaminations. The time-related profile of the excitation used is one of the main photothermal experiment characteristics. Considering a pulse (as close to a Dirac as possible), the experiment is called "pulsed method", better known as "flash method" [1,2]. This method is very efficient: the sample response contains all the frequencies of interest. However, using this technique, a high quantity of energy is deposited during a very short time. Thus, analyzing fragile materials with the flash method is impossible. In opposition, with a periodic excitation (for a given frequency), one speaks of "modulated method". The sample response is recorded using a lock-in amplifier. In this case, energetic stresses are smaller but a steady state has to be reached to begin measurements. The obtained response contains only one frequency component and, as a consequence, one needs to repeat the experiment on several occasions to carry out the complete study of a given sample material.

The last born of the photothermal methods, called "random method", uses a pseudo random binary signal (PRBS) as excitation [3]. Usually, the thermophysical properties of a given sample material are estimated thanks to well-known methods [4,5], after rebuilding its impulse response using a correlation analysis technique or an auto-regressive/auto-regressive moving average (AR/ARMA) model [6]. During the last decades, many approaches have been suggested for thermophysical properties estimation. One can classify these approaches into two main families: analytical approaches and heuristic approaches. Analytical approaches use gradient-based algorithms and need the derivatives of an objective function to be evaluated in order to identify unknown parameters (properties) [7–9]. However, most of the time, such algorithms only enable a local solution (and not the global one) to be found [10,11]. In addition, they can show instabilities leading to non-convergence, in case of correlated parameters. As a result, such approaches are restricted to the simultaneous estimation of uncorrelated parameters. In addition, computation time to reach a given precision can be large. The second family deals with heuristic approaches. Heuristic approaches are global search approaches and the most widely used heuristic algorithms are genetic (or evolutionary) algorithms [12,13]. Genetic algorithms are probabilistic search techniques based on the principles of genetics. Using these techniques, an objective function can be minimized without calculating derivatives. In addition, these algorithms do not easily fall into local minima and have demonstrated their robustness and efficiency. However, some optimization problems (called variant problems) cannot be solved by means of genetic

[a] e-mail: jean-luc.bodnar@univ-reims.fr

algorithms, due to poorly designed fitness functions. In addition and because of significant response times, genetic algorithms are not always well adapted to real-time applications. That is why the main objective of the present work was to develop an artificial-intelligence-based approach dealing with thermophysical properties estimation (thermal diffusivity and conductivity) from front-face or rear-face photothermal responses to a PRBS. As a key point, we demonstrated in a previous study [14] that rebuilding the impulse response of a material is not necessary when using AI tools. The new and "intelligent" approach we propose is based on side-by-side feedforward (multilayer) neural networks trained with the cascade-correlation algorithm [15–17]. The proposed estimation approach is computationally tractable and, as a result, implementable in an embedded system with limited CPU and memory resources.

Feedforward (multilayer) artificial neural networks (ANN) are known as universal and parsimonious approximators [18] and widely used to model and control complex non-linear systems [19–25]. They present some very interesting attributes, mostly their learning and generalization abilities, to be used as efficient estimation tools. However, such tools have to be trained using examples. That is why we used a database composed of 192 fictive materials to train the considered networks and focused on the impact of both the examples used during training and the number of hidden neurons (related to the number of parameters to be identified) on generalization. Generalization is about extracting key features from training data and using these features to produce appropriate outputs in response to inputs (photothermal responses) never experienced before (test phase).

The next section of the present paper (Sect. 2) is about the design of the proposed "neural" estimation approach. Then, the feedforward artificial neural networks used as well as the cascade-correlation algorithm are described. The following section (Sect. 3) focuses on the simulated data provided by the GRESPI laboratory of University of Reims Champagne-Ardenne (France) we used to develop and test the just-mentioned approach. In this section, we discuss also the results we obtained about thermophysical properties estimation. The paper ends with a conclusion and an outlook to future works.

2 The "neural" estimation approach

The proposed estimation approach is depicted by Figure 1 and formalized by equations (1) and (2). Two side-by-side feedforward artificial neural networks, trained with the cascade-correlation (CC) algorithm, are used to estimate simultaneously the thermal diffusivity and conductivity of a material M, from its front-face $\left(R^{\mathrm{FFm}}_{\mathrm{PRBS}}\right)$ or rear-face $\left(R^{\mathrm{RFm}}_{\mathrm{PRBS}}\right)$ photothermal response to a PRBS:

$$\begin{aligned} a_M &= \mathrm{ANN}^{\mathrm{FF}}_{1/2}\left(R^{\mathrm{FFm}}_{\mathrm{PRBS}}\right) \text{ and} \\ \lambda_M &= \mathrm{ANN}^{\mathrm{FF}}_{2/2}\left(R^{\mathrm{FFm}}_{\mathrm{PRBS}}\right), \forall M \text{ a material,} \end{aligned} \tag{1}$$

$$\begin{aligned} a_M &= \mathrm{ANN}^{\mathrm{RF}}_{1/2}\left(R^{\mathrm{RFm}}_{\mathrm{PRBS}}\right) \text{ and} \\ \lambda_M &= \mathrm{ANN}^{\mathrm{RF}}_{2/2}\left(R^{\mathrm{RFm}}_{\mathrm{PRBS}}\right), \forall M \text{ a material,} \end{aligned} \tag{2}$$

with a_M and λ_M the thermal diffusivity and conductivity of a material M, $\mathrm{ANN}^{\mathrm{FF}}_{1/2}$ and $\mathrm{ANN}^{\mathrm{FF}}_{2/2}$ the front-face neural estimation models and, finally, $\mathrm{ANN}^{\mathrm{RF}}_{1/2}$ and $\mathrm{ANN}^{\mathrm{RF}}_{2/2}$ the rear-face neural estimation models. As highlighted in [12], one can estimate directly thermophysical properties from this kind of response, using artificial intelligence tools (artificial neural networks or neuro-fuzzy systems). It means that, in opposition to what is usually done with standard approaches, rebuilding the impulse response of a given material is not necessary in order to characterize it. Feedforward artificial neural networks proved to be able,

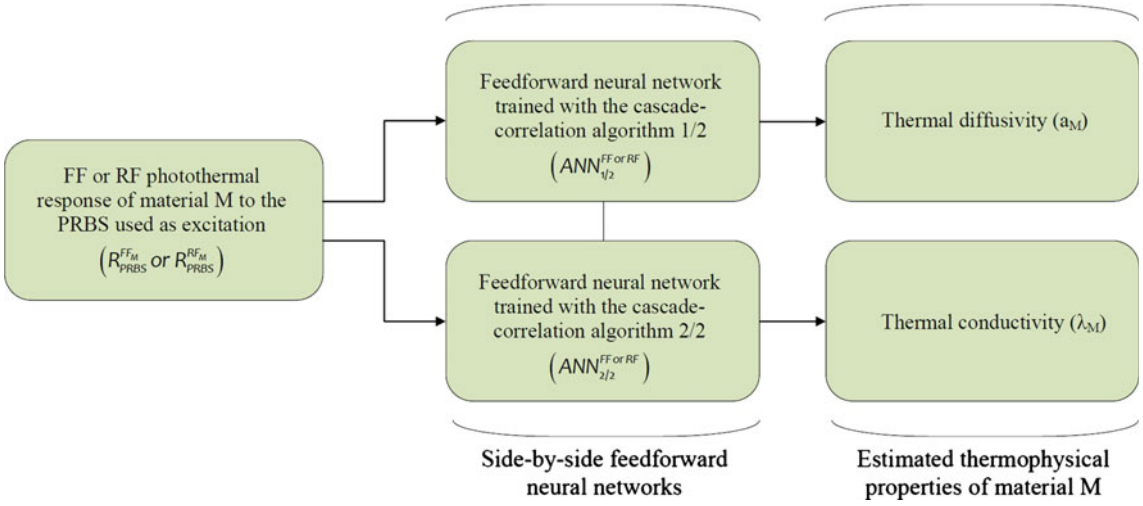

Fig. 1. The "neural" estimation approach. Estimation of the thermal diffusivity and conductivity from front-face $\left(R^{\mathrm{FFm}}_{\mathrm{PRBS}}\right)$ or rear-face $\left(R^{\mathrm{RFm}}_{\mathrm{PRBS}}\right)$ photothermal responses.

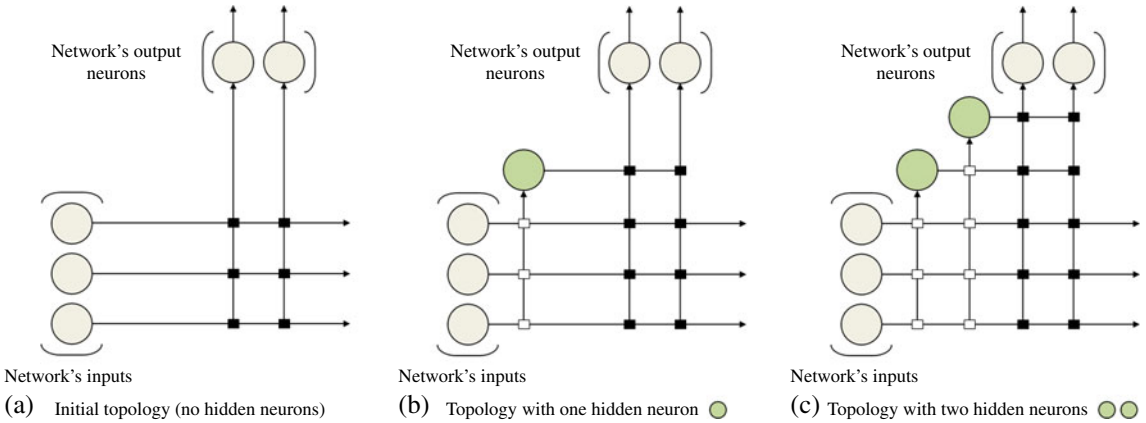

Fig. 2. The cascade-correlation algorithm. Black rectangles depict weighted connections between the network's inputs and output neurons or between hidden neurons and output neurons. White rectangles depict weighted connections between the network's inputs and hidden neurons or between hidden neurons [15–17].

after an appropriate training phase, to extract thermophysical properties of materials from photothermal responses. So, such an estimation approach allows limitations of correlation analysis techniques [6] to be avoided. Moreover and as previously mentioned in the paper, inverse methods are unable to estimate simultaneously two or more parameters in case of high correlation. Finally, the "single-parameter" (thermal diffusivity) approaches proposed and tested in [12] proved to be efficient, whatever the thermal behavior. The new "intelligent" estimation approach described in this paper strives to meet the same objective.

As it is well known, training algorithms based on gradient calculation are commonly used when developing nonlinear black-box models or estimation approaches using artificial intelligence tools. As stated in Section 1, gradient-based algorithms are unable to estimate simultaneously two or more parameters (thermophysical properties) in case of high correlation. However, the way artificial neural networks can be structured is a big advantage over the "standard" approaches. In the proposed "neural" estimation approach, each network is a "branch" of the same structure and can be trained independently from the other network. As a result, each "branch" of the neural structure allows one of the two correlated thermophysical properties we consider to be accurately estimated after a specific and effective training phase, without being impacted by correlation at all.

3 The cascade-correlation algorithm

During the past decade, artificial neural networks have been widely used to solve complex real-world problems. A key point when using such tools is first to find the appropriate topology of the networks used to solve a given problem (basically, the number of hidden layers as well as the number of units, or neurons, to be put on them) and, secondly, to optimize their parameters using training examples. Training aims at establishing a satisfactory relationship between input and output patterns. The cascade-correlation algorithm is an adaptive (or constructive) learning algorithm used with self-growing feedforward neural networks (with one hidden layer only, what proved to be enough to approximate a large class of functions). One speaks of "cascade-correlation neural networks" [15–17].

Compared with feedforward neural networks trained with the conventional backpropagation algorithm [26], cascade-correlation neural networks do not have a fixed size (i.e., a fixed number of units in the hidden layer). A cascade-correlation neural network grows from an initial topology with no hidden units. Each input is so connected to each output neuron and the network is trained using learning data (examples). These data have to be fully representative of all the features the network is intended to learn. When there is no significant reduction in the approximation error, the training phase is terminated and all the weights obtained are frozen. Then, hidden units will be dynamically added and trained one by one until a given performance criterion is satisfied (Fig. 2). Usually, a new hidden neuron is chosen from a pool of candidates with different initial weights. The new hidden units are so cascaded with the neural network inputs as well as existing hidden units. During the training process, the weights affected to the connections between these new units and both the network's inputs and preexisting hidden units ("input" weights) are adjusted by maximizing C, which is the sum over all the network's output neurons of the magnitude of the correlation between V_p, the value of the candidate unit for example p, and $E_{p,o}$, the residual output error measured at neuron o. A gradient ascent is performed to maximize C, with C expressed as follows (3):

$$C = \sum_{o} \left| \sum_{p} \left(V_p - \overline{V}\right) \left(E_{p,o} - \overline{E}_o\right) \right|, \tag{3}$$

$\overline{V}$ and $\overline{E}_o$ are the respective averaged values of V and E_o over all the available training examples. In order to maximize C (3), the partial derivative of C with respect

Table 1. The 192 fictive materials, a and λ are the thermal diffusivity ($m^2\ s^{-1}$) and conductivity ($W\ m^{-1}\ K^{-1}$).

Thermal conductivity (λ) \ Thermal diffusivity (a)	1×10^{-8}	5×10^{-8}	1×10^{-7}	5×10^{-7}	1×10^{-6}	5×10^{-6}	1×10^{-5}	5×10^{-5}
0.5	M01	M02	M03	M04	M05	M06	M07	M08
1	M09	M10	M11	M12	M13	M14	M15	M16
5	M17	M18	M19	M20	M21	M22	M23	M24
10	M25	M26	M27	M28	M29	M30	M31	M32
15	M33	M34	M35	M36	M37	M38	M39	M40
20	M41	M42	M43	M44	M45	M46	M47	M48
25	M49	M50	M51	M52	M53	M54	M55	M56
30	M57	M58	M59	M60	M61	M62	M63	M64
35	M65	M66	M67	M68	M69	M70	M71	M72
40	M73	M74	M75	M76	M77	M78	M79	M80
45	M81	M82	M83	M84	M85	M86	M87	M88
50	M89	M90	M91	M92	M93	M94	M95	M96
55	M97	M98	M99	M100	M101	M102	M103	M104
60	M105	M106	M107	M108	M109	M110	M111	M112
65	M113	M114	M115	M116	M117	M118	M119	M120
70	M121	M122	M123	M124	M125	M126	M127	M128
75	M129	M130	M131	M132	M133	M134	M135	M136
80	M137	M138	M139	M140	M141	M142	M143	M144
85	M145	M146	M147	M148	M149	M150	M151	M152
90	M153	M154	M155	M156	M157	M158	M159	M160
95	M161	M162	M163	M164	M165	M166	M167	M168
100	M169	M170	M171	M172	M173	M174	M175	M176
105	M177	M178	M179	M180	M181	M182	M183	M184
110	M185	M186	M187	M188	M189	M190	M191	M192

to each of the incoming weights of the candidates (w_i) has to be computed. $\partial C/\partial w_i$ can be expressed as follows (4):

$$\partial C/\partial w_i = \sum_{p,o} \sigma_o \left(E_{p,o} - \overline{E}_o\right) f'_p I_{i,p}, \tag{4}$$

σ_o is the correlation between the value of the candidate unit and output o, f'_p is the derivative of the candidate's activation function with respect to the sum of its inputs (for example p), $I_{i,p}$ is the input received by the candidate unit from unit i (for example p). When the process described above is finished, the adjusted "input" weights are also frozen. Weights affected to the connections between the new hidden units and output neurons (called "output weights") are further updated using the above-mentioned backpropagation algorithm with the aim of minimizing the network output error. This iterative procedure is of involving more and more hidden neurons is repeated so as to achieve a satisfactory approximation performance [8,9] (in our case, a good estimation of both the thermal diffusivity and conductivity of the studied materials).

4 Development phase and test

This section of the paper is about the training and test of the side-by-side feedforward artificial neural networks used as estimation tools. The simulated data used as well as the results we obtained about thermophysical properties estimation (from front-face or rear-face thermogram) are discussed.

4.1 Simulated data

As previously mentioned in the paper, the side-by-side feedforward neural networks used to estimate thermophysical properties have to be trained using examples. As a result, they will be able to extract both the thermal diffusivity and conductivity from photothermal responses to PRBS. The number of training examples and the relevance of these examples are key points when developing models or approximating functions with such tools. The training phase aims at finding the right topology of neural network and optimizing its parameters. The thermal behavior of homogeneous materials is related to thermal diffusivity and effusivity. This late thermophysical property can be replaced by the thermal conductivity. So, we used the simulated front-face and rear-face photothermal responses of 192 fictive materials (M01 to M192) to develop and test the new "intelligent" characterization approach we propose. Their thermal diffusivities (a) and conductivities (λ) range from 1×10^{-8} to 5×10^{-5} $m^2\ s^{-1}$ and from 0.5 to 110 $W\ m^{-1}\ K^{-1}$, respectively (Tab. 1). Thickness is 5 mm. In order to highlight the way the just-mentioned thermophysical properties impact on the photothermal response of a given material, we focus on three of the fictive materials: M01, M08 and M192 (Fig. 3). Taking a look at Figure 3 (each front-face photothermal response is normalized between 0 and 1), one can see that an increase in thermal diffusivity (M01 → M08, the thermal conductivity remains the same) leads to higher relative variability in the response. Its maximum value is also higher. In opposition, an increase in thermal conductivity

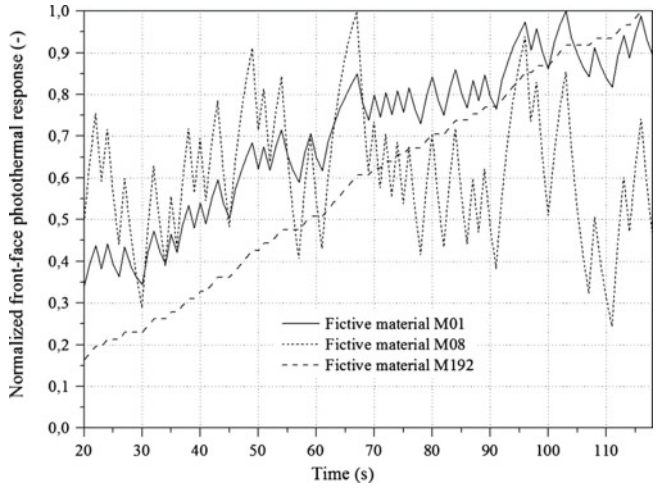

Fig. 3. Normalized front-face photothermal responses of the materials M01, M08 and M192.

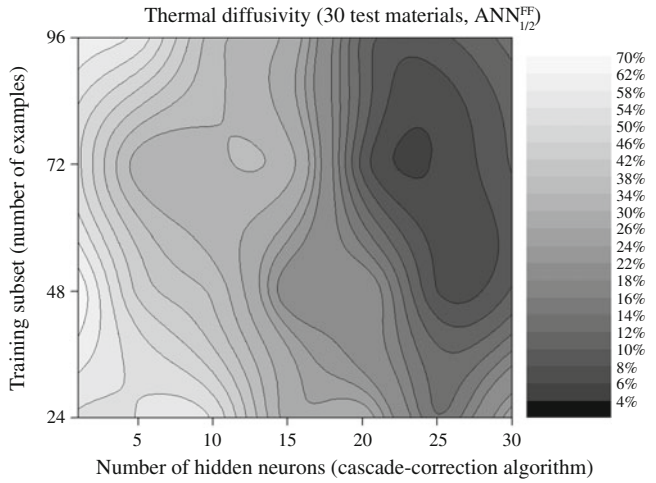

Fig. 4. Impact on generalization of the subset used during training and the number of hidden neurons. Mean relative error over the 30 test materials about thermal diffusivity estimation.

(M01 → M192, the thermal diffusivity remains the same) leads to lower relative variability in the response as well as a lower maximum value. In light of those observations, we built the database of 192 fictive materials presented by Table 1. With such a database, all the thermal behaviors of interest can be presented to the side-by-side feedforward artificial neural networks ("neural" estimation approach) used during both the training and test phases.

Let us highlight that, in addition to the research for the topology of the tools used, the way the considered tools are trained and validated is another key point. That is why we considered four training subsets composed of 24 (highlighted in yellow in Tab. 1), 48 (adding to the first subset the examples highlighted in green in Tab. 1), 72 (adding to the second subset the examples highlighted in blue in Tab. 1) and 96 materials (adding to the third subset the examples highlighted in grey in Tab. 1), respectively. Our objective is to find the adequate subset of examples to be used during the training phase. The test subset is composed of 30 materials and enables generalization to be evaluated (highlighted in pink in Tab. 1). As it can be noticed when looking at Table 1, the training and test subsets are built in a way that reflects the diversity of the thermal characteristics materials can have. Generalization is about extracting key features from the training data and using these features to produce appropriate outputs in response to inputs never experienced before (i.e., inputs that are not part of the training subset used to identify the parameters of the model). As a consequence, training examples have to bring enough information to the feedforward neural networks used to approximate the underlying function to the desired degree of accuracy. However, too many examples to learn (with possibly redundant examples) can lead to over parameterized models (because of a substantial increase in the number of hidden neurons) and, as a consequence, a poor generalization ability. In addition, the higher the number of hidden neurons, the higher the computation time. As a result, the optimal topology of the tools used has to be found (i.e., the optimal number of hidden neurons, related to the number of model parameters) on the basis of a compromise between training examples, generalization ability and computation time. Let us remember that the proposed algorithms about thermophysical properties estimation have to be computationally tractable to be usable in situ when making cartography of a medium.

4.2 Thermophysical properties estimation with the "neural" estimation approach

This section is about the optimization of the side-by-side feedforward neural networks used and the results we obtained when estimating thermal diffusivity and conductivity. We focused on the impact on generalization of both the number of examples used during training and the number of hidden neurons, leading to a number of parameters to be identified. The test subset (30 materials) enable generalization to be evaluated.

4.2.1 Estimation of thermal diffusivity and conductivity from front-face photothermal responses

Figures 4 ($ANN^{FF}_{1/2}$) and 5 ($ANN^{FF}_{2/2}$) highlight the way the cascade-correlation learning algorithm checked generalization during training, on the basis of the number of examples used and the number of hidden neurons (related to the number of model parameters to be identified from the simulated data). Let us remember that the cascade-correlation algorithm is an adaptive (or constructive) learning algorithm used with self-growing feedforward neural networks. So, a network grows from an initial topology with no hidden neurons (each input is so connected to each output neuron) and new units are dynamically added and trained one by one until a given performance criterion (related to generalization) is satisfied.

Table 2. Estimation of the thermal diffusivity (a) and conductivity (λ) from simulated front-face photothermal responses. Mean relative error over the 30 test materials.

Estimation of thermal diffusivity and conductivity from simulated front-face photothermal responses					
Model	Training examples	Hidden neurons	Mean relative error (%)	Minimum error (%)	Maximum error (%)
$ANN^{FF}_{1/2}$	72 (subset 3)	24	6.2	3.4	9.6
$ANN^{FF}_{2/2}$	72 (subset 3)	20	7.3	3.7	10.9

Taking a look at Figure 4, one can see that generalization is the best when considering the third training subset (composed of 72 examples) and 24 hidden neurons ($ANN^{FF}_{1/2}$). With such a configuration, the mean relative error about thermal diffusivity estimation (over the 30 materials considered during the test phase) is about 6.2% (Tab. 2). As one can see in Figure 4, error is high when the number of hidden neurons is low (in this case the network is underparameterized, what hinders learning), whatever the training subset used, and decreases as the cascade-correlation algorithm adds new neurons to the network. In opposition, when the number of hidden neurons is too high (higher than 25), the network's generalization ability decreases (in this case the network is overparameterized, what leads to overfitting) and, as a result, the learning phase is stopped. Considering the fourth training subset (composed of 96 materials) and 25–30 hidden neurons, estimation results are pretty good (the mean relative error is about 8–10%) but the 24 examples added to the third subset do not bring more usable information to the network. Clearly, this new information is (at least partially) redundant what makes harder the extraction from the training data of the key features allowing good estimates of thermal diffusivity to be produced.

Taking a look at Figure 5, one can remark that generalization is the best when considering again the third training subset and only 20 hidden neurons ($ANN^{FF}_{2/2}$). Using this configuration, the mean relative error about thermal conductivity estimation is about 7.3% (Tab. 2). The same remarks as for model $ANN^{FF}_{1/2}$ apply for model $ANN^{FF}_{2/2}$: whatever the training subset, estimation of thermal conductivity is poor in case of a too low number of neurons while it is pretty good (the mean relative error is about 8–10%) using at least 17–18 hidden units. Again, when considering the fourth training subset, more hidden neurons are needed (between 25 and 30) to obtain satisfactory (but of course not optimal) results.

As a first conclusion, both the thermal diffusivity and conductivity of a given material can be estimated simultaneously from its front-face photothermal response to a PRBS with efficiently trained (using the cascade-correlation algorithm) side-by-side feedforward neural networks. This allows computation time (about 150 ms when using a personal computer equipped with an Intel Core i7-2760 QM at 2.4 GHz processor, 8 GB of RAM, and Microsoft Windows 7, 64 bits) to be significantly reduced in comparison to the time needed by standard approaches. As a key point, estimation of thermal diffusivity requires more hidden neurons (24 vs. 20, i.e., +20%), and as a result more model parameters, than estimation of thermal conductivity. Let us remember that thermal diffusivity is defined as the ratio of thermal conductivity to volumetric heat capacity. Thermal diffusivity deals with thermal inertia and, as a result, is related to heat conduction and storage. Thermal conductivity is only about heat conduction. This can explain why, considering the same number of training examples (i.e., 72), more hidden neurons are needed to estimate thermal diffusivity accurately.

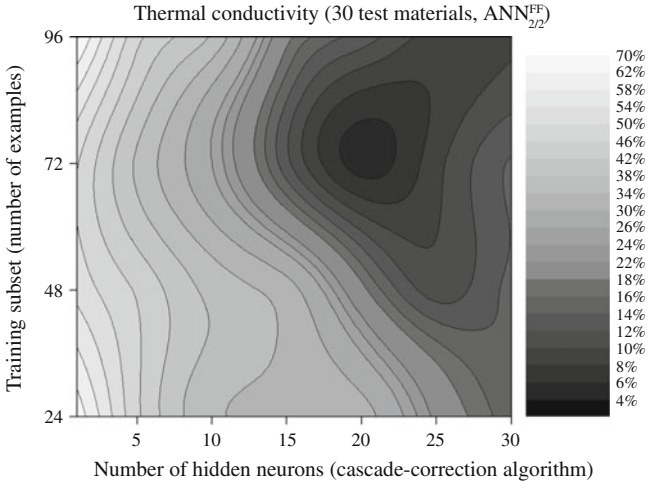

Fig. 5. Impact on generalization of the subset used during training and the number of hidden neurons. Mean relative error over the 30 test materials about thermal conductivity estimation.

4.2.2 Estimation of thermal diffusivity and conductivity from rear-face photothermal responses

Taking a look at Figures 6 and 7 (the thermal diffusivity and conductivity of the considered materials are estimated from rear-face photothermal responses), one can see that generalization is optimal when considering in both cases the third training subset and 26 ($ANN^{RF}_{1/2}$) or 21 ($ANN^{RF}_{2/2}$) hidden neurons, respectively. Using these configurations, the mean relative error over the 30 test materials we considered is about 5.8 and 6.1%, respectively (Tab. 3). Again, estimation of thermal diffusivity requires more hidden neurons (26 vs. 21, i.e., +25%), and as a result more parameters, than estimation of thermal conductivity. Computation time is also slightly higher (about 200 ms) but the proposed approach remains

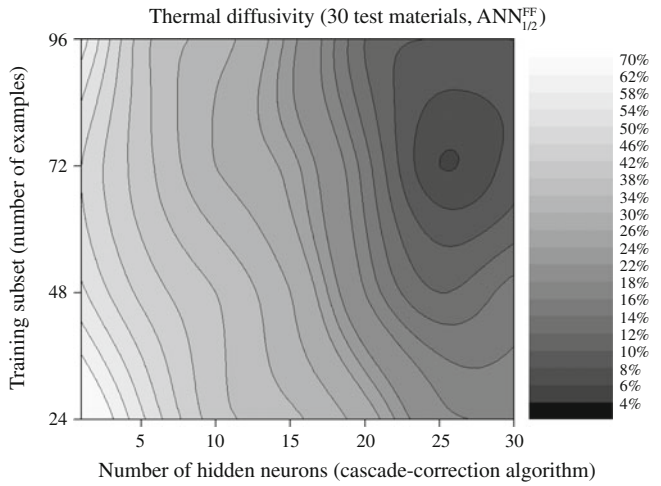

Fig. 6. Impact on generalization of the subset used during training and the number of hidden neurons. Mean relative error over the 30 test materials about thermal diffusivity estimation.

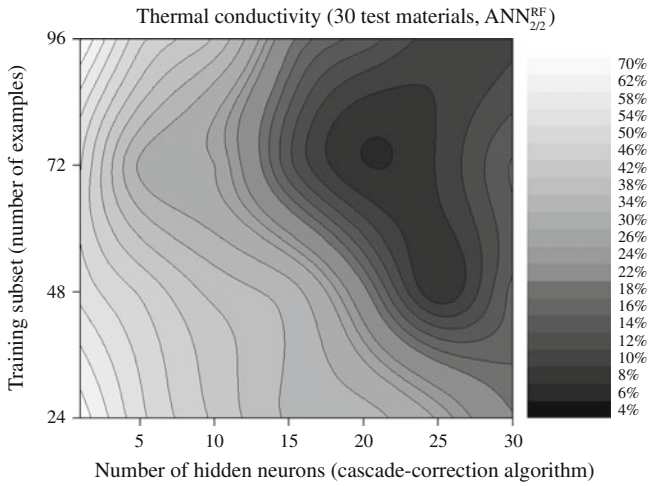

Fig. 7. Impact on generalization of the subset used during training and the number of hidden neurons. Mean relative error over the 30 test materials about thermal conductivity estimation.

computationally tractable. The third subset (composed of 72 examples) remains the optimal training subset. Again, the results highlight that both thermophysical parameters can be simultaneously estimated with good accuracy (even though accuracy is slightly better for thermal diffusivity) from rear-face photothermal responses to a pseudo random binary signal using efficiently trained side-by-side feedforward neural networks. Finally, when comparing the estimation results we obtained from front-face and rear-face photothermal responses, one can note that estimation of thermal diffusivity and conductivity from rear-face responses is more accurate than when using front-face responses. The mean relative error over the 30 test materials is reduced of about 6.5% with model $ANN^{RF}_{1/2}$ (in comparison to the results provided by model $ANN^{FF}_{1/2}$) and 16.5% with model $ANN^{RF}_{2/2}$ (in comparison to the results we obtained with model $ANN^{FF}_{2/2}$).

Taking a look at the results we obtained about thermal diffusivity (a) and conductivity (λ) estimation, one can highlight that the mean relative error over the 30 test materials is slightly higher for thermal conductivity than for thermal diffusivity. In addition, for both thermophysical properties, "rear-face" estimates (estimates from simulated rear-face photothermal responses) are more accurate than "front-face" estimates (estimates from simulated front-face photothermal responses). Thermal conductivity shows the ability of a material to conduct heat while thermal diffusivity determines how rapidly heat will flow within it. So, thermal diffusivity is related to transient heat transfer while thermal conductivity is about stationary phenomena. As a key point, we subjected homogeneous materials to a pseudo random binary signal and we obtained photothermal transient responses. As a result, this kind of photothermal response is better adapted to the estimation of thermal diffusivity (or thermal effusivity) than thermal conductivity. This can explain why we obtained better estimates for thermal diffusivity, whatever the considered photothermal responses (front-face or rear-face photothermal responses).

5 Conclusion

In the present paper, an artificial-intelligence-based approach dealing with the estimation of thermophysical properties (the thermal diffusivity and conductivity) is designed and evaluated. This new and "intelligent" approach makes use of photothermal responses obtained when subjecting homogeneous materials to a light flux. Previous studies have shown all the interest in considering an excitation with a random-time profile, notably in case of fragile materials to be characterized. Usually, the properties of a homogeneous material can be estimated thanks to gradient-based algorithms, after rebuilding its impulse response using a correlation

Table 3. Estimation of the thermal diffusivity (a) and conductivity (λ) from simulated rear-face photothermal responses. Mean relative error over the 30 test materials.

Estimation of thermal diffusivity and conductivity from simulated rear-face photothermal responses					
Model	Training examples	Hidden neurons	Mean relative error (%)	Minimum error (%)	Maximum error (%)
$ANN^{RF}_{1/2}$	72 (subset 3)	26	5.8	2.9	8.5
$ANN^{RF}_{2/2}$	72 (subset 3)	21	6.1	3.2	8.7

analysis technique or an auto-regressive/auto-regressive moving average (AR/ARMA) model. As it is well known, correlation among unknown parameters (properties) impacts negatively gradient-based estimation approaches. As a result, such analytical approaches are restricted to the simultaneous estimation of uncorrelated thermophysical properties. Moreover, in some cases, an order of magnitude among all of the parameters to be identified is needed by such algorithms and computation time can be large to reach a given precision. That is why the main objective of the present work was to develop an alternative (to standard ones) approach dealing with the simultaneous estimation of thermal diffusivity and conductivity from front-face or rear-face photothermal responses to a pseudo random binary signal (PRBS). As we demonstrated previously, rebuilding the impulse response of a material to be characterized is not necessary. The proposed approach is based on side-by-side feedforward artificial neural networks trained with the cascade-correlation algorithm. This constructive learning algorithm allows the right topology of the tools used to be found dynamically and favors generalization. Artificial neural networks present some very interesting attributes, mostly their learning and generalization abilities, and can be used as efficient estimation tools.

A key point in using artificial neural networks is training. The training phase aims at finding the right topology of the tool used and optimizing its parameters. That is why we focused on the impact on generalization of both the number of examples used during training and the number of hidden neurons and highlighted optimal configurations (i.e., configurations leading to the best accuracy in thermal diffusivity and conductivity estimates). As a conclusion, we developed a new and "intelligent" approach capable of estimating both the thermal diffusivity and conductivity of homogeneous materials with very good accuracy (the mean relative error over the 30 test materials we considered ranges between 5% and 7%, whatever the considered photothermal response). In addition, the developed estimation algorithms are computationally tractable. Future work will first focus on confronting the proposed approach with noisy simulated data in order to evaluate the impact of noise on performance. Then the approach will be validated using experimental data. Finally, we will focus on characterizing two-layer materials and locating/identifying structural defects.

References

1. K.D. Maglic, A. Cezairliyan, V.E. Peletsky, *Compendium of Thermophysical Property Measurement Methods 1: Survey of Measurement Techniques* (Plenum Publishers, New York, USA, 1984)
2. K.D. Maglic, A. Cezairliyan, V.E. Peletsky, *Compendium of Thermophysical Property Measurement Methods 2: Recommended Measurement Techniques and Practices* (Plenum Publishers, New York, USA, 1992)
3. J.L. Bodnar, S. Brahim Djelloul, A. Boutemy, J.C. Cantone, P. Grossel, Contrôle non destructif par radiométrie photothermique sous excitation aléatoire : principe et exemples d'application, Congrès Annuel de la Société Française de Thermique, Reims, France, 2005
4. J.V. Beck, K.J. Arnold, *Parameters Estimation in Engineering and Sciences* (Wiley Ed., USA, 1977)
5. D. Maillet, D. Petit, Techniques inverses et estimations de paramètres, Techniques de l'Ingénieur, TI AF4515 and AF4516, 2008
6. S. Brahim Djelloul, Ph.D. thesis, University of Reims Champagne-Ardenne, France, 2008
7. O. Faugeroux, B. Claudet, S. Bénet, J.J. Serra, D. Boisson, International Journal of Thermal Sciences **43**, 383 (2004)
8. F. Mzali, L. Sassi, A. Jemni, S. Ben Nasrallah, Journal of High Temperatures-High Pressures **35/36**, 281 (2003/2004)
9. F. Albouchi, M. Fetoui, F. Rigollet, M. Sassi, S. Ben Nasrallah, International Journal of Thermal Sciences **44**, 1090 (2005)
10. J.F. Bonnans, J.C. Gilbert, C. Lemaréchal, C.A. Sagastizabal, *Numerical Optimization*, Theoretical and Practical Aspects Series (Springer-Verlag Ed., Deutschland, 2006)
11. J.A. Snyman, *Practical Mathematical Optimization: an Introduction to Basic Optimization Theory and Classical and New Gradient-Based Algorithms*, Applied Optimization (Springer-Verlag Ed., Deutschland, 2005)
12. S.N. Sivanandam, S.N. Deepa, *Introduction to Genetic Algorithms* (Springer-Verlag Ed., Deutschland, 2008)
13. D. Goldberg, *Genetic Algorithms in Search, Optimization, and Machine Learning* (Addison-Wesley Ed., USA, 1989)
14. S. Grieu, O. Faugeroux, A. Traoré, B. Claudet, J.-L. Bodnar, Energy Build. **43**, 543 (2011)
15. S. Fahlman, C. Lebiere, in *Advances in Neural Information Processing systems*, edited by D.S. Touretzky et al., vol. 2 (Morgan Kaufmann, Los Altos, USA, 1990), pp. 524–532
16. D.S. Phatak, I. Koren, IEEE Trans. Neural Netw. **5**, 930 (1994)
17. J.K. Spoerre, Comput. Ind. **32**, 295 (1997)
18. K. Hornik, M. Stinchcombe, H. White, Neural Netw. **2**, 359 (1989)
19. H. Ohno, T. Suzuki, K. Aoki, A. Takahasi, G. Sugimoto, Neural Netw. **7**, 1303 (1994)
20. K.P. Venugopal, A.S. Pandya, R. Sudhakar, Neural Netw. **7**, 833 (1994)
21. I. Flood, P. Christopholis, Autom. Constr. **4**, 307 (1996)
22. S. Grieu, A. Traoré, M. Polit, J. Colprim, Eng. Appl. Artif. Intell. **18**, 559 (2005)
23. S. Grieu, F. Thiéry, A. Traoré, T.P. Nguyen, M. Barreau, M. Polit, Chem. Eng. J. **116**, 1 (2006)
24. W.J. Zhang, C.J. Bai, G.D. Liu, Ecol. Modell. **201**, 317 (2007)
25. Y. Zuo, Y. Wang, X. Liu, S.X. Yang, L. Huang, X. Wu, Z. Wang, Appl. Math. Model. **34**, 1823 (2010)
26. C. Charalambous, IEEE Proc. **139**, 301 (1992)